Chemical Engineering Journal 165 (2010) 490–499

Contents lists available at ScienceDirect

Chemical Engineering Journal

journal homepage: www.elsevier.com/locate/cej

Mechanism investigation of catalyzed ozonation of 2-methylisoborneol in drinking water over aluminum (hydroxyl) oxides: Role of surface hydroxyl group

Fei Qi[a,b,*], Bingbing Xu[c], Zhonglin Chen[b,1], Liqiu Zhang[a], Panyue Zhang[a], Dezhi Sun[a]

[a] College of Environmental Science and Engineering, Beijing Forestry University, Beijing 100083, PR China
[b] State Key Laboratory of Urban Water Resource and Environment, Harbin Institute of Technology, Harbin 150090, PR China
[c] State Environmental Protection Key Laboratory for Lake Pollution Control, Chinese Research Academy of Environmental Sciences, Beijing 100012, PR China

ARTICLE INFO

Article history:
Received 11 May 2010
Received in revised form 3 September 2010
Accepted 10 September 2010

Keywords:
Aluminum hydroxyl oxide
2-Methylisoborneol
Catalyzed ozonation
Hydroxyl radical
Adsorption

ABSTRACT

In this investigation, the mechanism of catalyzed ozonation of MIB by aluminum oxides (γ-AlOOH and γ-Al_2O_3) was studied. It was concluded that the roles of surface hydroxyl groups in adsorption and catalyzed ozonation determined catalyzed ozonation mechanism. The removal efficiency of MIB in catalyzed ozonation by γ-Al_2O_3 or γ-AlOOH was 98.4% and 27.5%, respectively. Effect of water pH on catalyzed ozonation indicated that surface hydroxyl group, of which surface net charge was zero, was the active site of catalysts. Radical scavenger experiments results indicated that catalyzed ozonation by γ-Al_2O_3 followed a hydroxyl radical (•OH) reaction-pathway and the reaction-pathway of catalyzed ozonation by γ-AlOOH followed solid surface mechanism. However, both γ-AlOOH and γ-Al_2O_3 can enhance ozone decomposition to generate hydroxyl radical in catalytic ozone decomposition (without MIB). The inconsistent results between radical scavengers and catalytic ozone decomposition were mainly due to the interaction between MIB and surface hydroxyl groups. According to MIB adsorption on γ-AlOOH or γ-Al_2O_3, MIB interacted with surface hydroxyl group by chemical adsorption, and surface hydroxyl group was the main adsorption site. The adsorption capability of γ-AlOOH was higher than that of γ-Al_2O_3. The participation of surface hydroxyl group in adsorption restrained its capability of catalyzed ozone decomposition to generating •OH. γ-AlOOH that was covered with more surface hydroxyl groups, adsorbed MIB more stronger and inhibited generation of •OH in catalyzed ozonation of MIB, resulting in lower removal efficiency of MIB in catalyzed ozonation. In addition, the surface texture and chemical properties of catalyst that can help to understand the catalyzed mechanism.

1. Introduction

The removal of taste and odor is showed great concern by the drinking water industry due to consumers' associate off-flavors with the poor drinking water quality [1]. Some of these off-flavor compounds have been identified as the secondary metabolic products of cyanobacteria and actinomycete that emerged in eutrophic water. 2-Methylisoborneol (MIB) is one of the most common taste and odor compounds, and always produce earthy and musty odor [2]. The threshold concentration of MIB in drinking water was reported as low as 4.0 ng L^{-1} [3]. This means that the water quality will be affected by MIB with very low concentration, and make people feel unpleasure. In order to remove MIB from the source water, several water treatment techniques including advanced treatment methods have been implemented. However, the results showed that the conventional drinking water treatment could not effectively remove MIB from water due to its special chemical property and the low threshold concentration. MIB could also be ineffectively degraded by chlorine, chlorine dioxide or potassium permanganate in the pre-oxidation process [4]. Though both of powder activated carbon (PAC) and granular activated carbon (GAC) can effectively remove MIB from water, there are some disadvantages in practice. In detail, too much activated carbon is asked for the treatment, and the residual sludge of activated carbon is difficult for disposal [5]. Therefore, it is necessary to explore an available advanced treatment technology to resolve taste and odor problems in drinking water.

It is well known that advanced oxidation processes (AOPs) is an effective way to decompose pollutants because of the generation of hydroxyl radical (•OH) as the predominant species. AOPs are attractive alternatives for the conventional water treatment and have received considerable attention in recent years [6]. Recently, several AOPs such as O_3/H_2O_2 [7], UV/H_2O_2 [8], photo-catalytic oxi-

* Corresponding author at: P.O. Box 60, No. 35 Qinghua East Road, Haidian District, Beijing City, PR China.
E-mail addresses: qifei@bjfu.edu.cn (F. Qi), zhonglinchen@263.net (Z. Chen).
[1] State Key Laboratory of Urban Water Resource and Environment, Harbin Institute of Technology, P.O. Box 2606, Harbin 150090, PR China.

1385-8947/$ – see front matter © 2010 Elsevier B.V. All rights reserved.
doi:10.1016/j.cej.2010.09.047

dation [9], and ultrasonic oxidation [10] have been investigated as the potential methods for MIB removal from the source water. Unfortunately, there are still some drawbacks that limit the application of these AOPs in water treatment plant, i.e. unsedimentation of TiO_2 powder, the short life of UV lamps and ultrasonic irradiation equipment and the disposal of the residual of H_2O_2. Ozonation is an effective option for the removal of taste and odor in drinking water. Ozone is unstable in water, and can decompose into an oxygen molecule and an oxygen atom that will not have negative impacts on the human body. However, the formation of the hazardous by-products (such as bromate, ketoaldehyde and fatty acid with low molecular weight) must be carefully deduced [11]. Recently, catalyzed ozonation was paid more attention to enhance the mineralization ability and decrease the formation of hazardous by-products during ozonation. Several researches focused on catalyzed ozonation in the presence of solid metal oxides to remove recalcitrant pollutants [12]. In addition, catalyzed ozonation have already been used for taste and odor compounds removal from water [13–16]. High removal efficiency and convenient application of catalyzed ozonation for taste and odor removal had been obtained, but the reaction mechanism had not been clarified yet.

In the catalyzed ozonation, the reaction mechanism is complex. It is a combination of the sole ozonation, adsorption and catalyzed reaction. According to the previous investigation, three possible pathways have been speculated [12]: (1) chemisorption of ozone on the catalyst surface leading to the formation of active species which can oxidize the non-chemisorbed organic molecule; (2) chemisorption of organic molecule (associative or dissociative) on the catalyst surface and its further oxidation by gaseous or aqueous ozone; (3) chemisorption of both ozone and organic molecules and the subsequent interaction between chemisorbed species. Accordingly, the surface acidity-alkalinity property of catalyst and the adsorption behavior between the model pollutant and catalyst play important roles in heterogeneous catalyzed ozonation. However, the catalyzed ozonation mechanism had been seldom explained according to the adsorption behavior between model pollutant and the catalyst in previous studies. As it may be an important reaction process, the adsorption behavior is crucial for heterogeneous catalyzed ozonation. The reaction pathway of heterogeneous catalyzed ozonation revealed by the adsorption behavior has a certain theoretical significance for selecting catalyst to remove special organic pollutants.

Based on the above, the aim of this research was neither to explore an effective catalyst to remove MIB, nor to investigate the sub-products of MIB in catalyzed ozonatioin. The main aim was to discuss the role of adsorption behavior between MIB and catalysts in catalyzed ozonation and to explain the effect of surface acidity-alkalinity property of different catalysts on catalyzed ozonation of MIB. Firstly, the characterization of the surface texture and acidity-alkalinity property of γ-AlOOH and γ-Al_2O_3 were studied. Then the removal efficiency and reaction kinetics of MIB by catalyzed ozonation in the presence of γ-AlOOH or γ-Al_2O_3 were investigated. Finally, the mechanism of catalyzed ozonation of MIB by aluminum oxides was interpreted by the interaction between surface hydroxyl group and MIB.

2. Experimental

2.1. Catalysts and chemicals

Aluminum (hydroxyl) oxides used as catalysts were synthesized using precipitation method in our laboratory. γ-AlOOH (HAO) was obtained by precipitating aluminum nitrate ($Al(NO_3)_3{\cdot}9H_2O$) with ammonia ($NH_3{\cdot}H_2O$) until water pH achieved 9.0. The suspension was aged at 30 °C for 10–15 days. After that, precipitates were rinsed with ultra-pure water (18 MΩ cm) repeatedly until the conductivity of the supernatant remained constant. After dried at 70 °C, HAO was obtained. γ-Al_2O_3 (RAO) was obtained by calcining the HAO at 450 °C for 4 h. The crystalline phases of the catalysts were confirmed to be γ-AlOOH and γ-Al_2O_3 by X-ray diffraction (XRD). The HAO and RAO were ground and screened. Aluminum oxides with diameter between 0.075 mm and 0.3 mm were used in experiments.

MIB was synthesized in our lab by the method described by Wood and Snoeyink [17]. The purity of synthesized MIB was above 95.0%, which was confirmed by Gas chromatography- Mass spectrum (GC-MS). The MIB stock solution was prepared by dissolving the synthesized MIB in Milli-Q ultra-pure water (18 MΩ cm). The water used throughout all experiments was produced by a Milli-Q ultra-pure water system. All chemicals used were of analytical or higher grade.

All glassware equipments used in the experiments were immersed in the solution of H_2SO_4–$K_2Cr_2O_7$ over night, and then washed by tap water and ultra-pure water for over three times, respectively.

2.2. Analytical methods

2.2.1. Characterization of surface texture, pH_{pzc} and the density of surface hydroxyl groups

Specific surface area, pore volume and average pore size of aluminum (hydroxyl) oxides, were analyzed by Surface Area and Porosity Analyzer (Micromeritics ASAP 2020 M, USA). Before nitrogen adsorption isotherms experiment, HAO and RAO was degassed at 70 °C for 6 h and at 300 °C for 6 h, respectively. The nitrogen adsorption isotherms experiment was carried out at 77 K. The specific surface area was determined by Brunauer–Emmett–Teller (BET) method and the pore size distribution of catalysts were determined by Barrett–Joyner–Halenda (BJH) method from the desorption branch of the isotherm of N_2. The point of zero charge (pH_{pzc}) of the catalyst was determined using the mass titration method described elsewhere [18]. $HClO_4$ solution (1.0 mmol L^{-1}) and NaOH solution (1.0 mmol L^{-1}) were used as the titrant for acidity titration and alkalinity titration, respectively. Three ionic strengths in the sample suspensions supported by the background electrolyte ($NaNO_3$) were 0.005, 0.05 and 0.5 mol L^{-1}. The density of the surface hydroxyl group was measured by Grignard method described by Tamura [19]. The surface hydroxyl group on metal oxides (–OH) reacts with methyl magnesium iodide (CH_3MgI) to evolve methane according to the following reaction (equation (1)). The density of surface hydroxyl group is determined based on the mass of methane.

$$-OH + CH_3MgI \rightarrow -OMgI + CH_4\uparrow \quad (1)$$

2.2.2. Dissolved ozone concentration and MIB

The dissolved ozone concentration was measured by using the indigo method [20]. MIB was analyzed by gas chromatography with flame ionization detector (GC-FID) followed by the extraction with n-pentane [21]. The method detection limit (MDL) for MIB was 60.0 ng L^{-1}, and the relative standard deviation (RSD) was below 5.0%. In this study, the experiments were all conducted in triplicate and the averages were given in figures.

2.3. Experimental procedures

The catalyzed ozonation with and without catalysts (HAO and RAO) runs were performed in the batch mode at an ambient temperature of 20 ± 2 °C. The glass reactor (1 L) that had been modified from a flat-bottomed flask was described in our previous research [15]. Ozone was produced by a laboratory ozonizer (DHX-SS-1G, Harbin Electrochemistry Engineering Ltd., China) supplied with the dry pure oxygen. The maximum ozone production of this ozonizer was 9 g h^{-1}. After the generator reached a steady state, ozone gas was bubbled into ultra-pure water in the reactor with a silica dispenser for a period to achieve a desired aqueous ozone concentration. Then, the ozone gas was shut off. And the catalyst and stock solution (1 mL) of MIB were immediately added into the reactor. At the same time, the magnetic stirrer was turned on. Samples were collected at predetermined time intervals and immediately analyzed. In this study, dissolved ozone concentration in the reactor was controlled by varying the oxygen flux, the voltage of the ozone production and the time at which ozone was introduced into the reactor. Because ozone was added into the reaction system in a one-off form, the concentration of dissolved ozone and MIB were attenuated during the reaction. The volatilization of ozone and MIB were ignored by using sealed reactor. The solution pH was adjusted with the phosphate buffer solution (0.1 mmol L^{-1}).

The sole ozone decomposition and catalyzed ozone decomposition experiments were carried out in the batch mode at ambient temperatures (20 ± 2 °C) in the same reactor. After the generator reached a steady state, ozone gas was bubbled into ultra-pure water in the reactor with a silica dispenser for a desired period to achieve a desired ozone concentration. Then, the ozone gas was shut off, and the catalyst was immediately dropped into the reactor. The magnetic stirrer was turned on to initiate the catalytic ozone decomposition reaction. Samples were withdrawn at predetermined time intervals, and the residual ozone was instantly quenched with indigo. The solution pH was adjusted with the phosphate buffer solution (0.1 mmol L^{-1}).

Batch isothermal adsorption experiments were carried out in glass vessels (20 mL) with screw caps. Glass vessels were filled with MIB solution. After equilibrium (equilibrium time = 1.0 h) in a reciprocating shaker under 24 ± 1 °C, aluminum oxides were added into glass vessels to achieve a concentration of 200 mg L^{-1}. The suspensions were continuously mixed on the shaker for 24 ± 0.1 h, and then filtrated with cellulose acetate ultra-filtration membrane (0.45 μm). The residual concentration of MIB in the supernatant was analyzed by GC-FID subsequently.

3. Results and discussion

3.1. Surface texture characteristics of aluminum (hydroxyl) oxides

Surface texture characteristics of aluminum (hydroxyl) oxides were carried out by N_2 adsorption and desorption method. Surface texture parameters of HAO and RAO were listed in Table 1. Generally, HAO is representative of hydrous aluminum oxide, and RAO is one of aluminum oxides in the medium temperature zone. After calcinations, both the specific surface area and the pore diameter of RAO were increased compared with HAO. The pore characteristics of catalysts were shown in Fig. 1. The pore diameter distribution of HAO was mainly in the range of 20–30 nm and 100–120 nm. However, the pore diameter distribution of RAO was quite different from that of HAO. The pore diameter distribution of RAO was mainly range from 20 to 110 nm, which was remarkable wider than that of HAO. The average pore diameter of RAO was slightly greater than that of HAO (shown in Table 1). The pore volume of RAO was significant higher than that of HAO.

In water, H_2O molecules are adsorbed on the surface of metal oxides and result in hydroxylation [22]. Thus, the hydroxyl groups covered the surface of aluminum oxides. The surface hydroxyl group was characterized by density of surface hydroxyl group (Table 1). It was clear that density of surface hydroxyl group decreased after the calcinations, resulting from the surface hydroxyl groups being stripped at the high temperature.

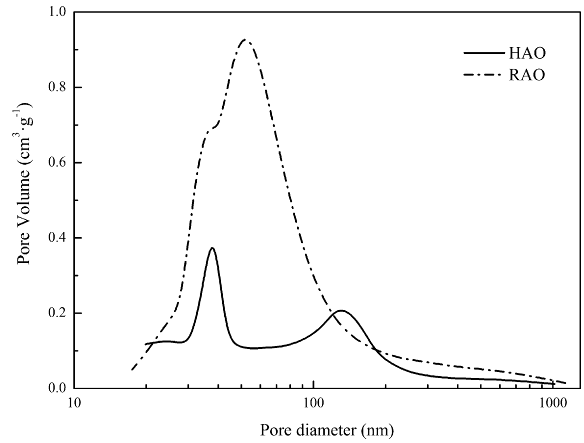

Fig. 1. Pore size distribution of aluminum oxides.

3.2. Surface acidity-alkalinity property of aluminum (hydroxyl) oxides

Generally, the surface of aluminum (hydroxyl) oxide exhibits an amphiprotic property (acidity and alkalinity). In this study, acidity-alkalinity titration was used to determine the surface acidity and alkalinity property of catalysts. As shown in Fig. 2, acidity-alkalinity

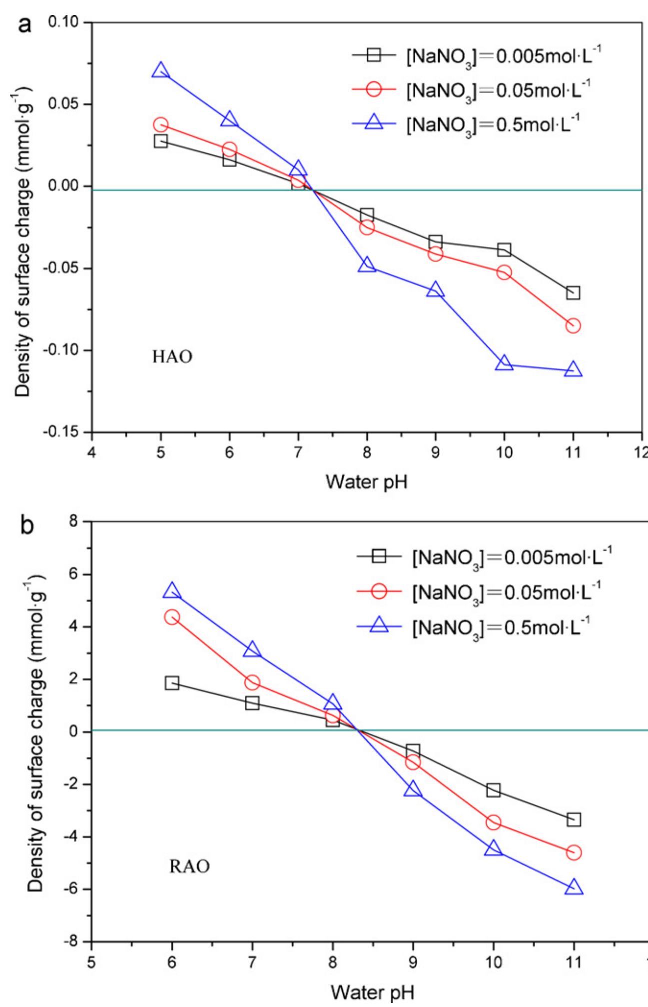

Fig. 2. Surface charge density – solution pH for γ-AlOOH and γ-Al_2O_3 (a) γ-AlOOH, (b) γ-Al_2O_3.

Table 1
Surface area, pore volume and pore diameter of aluminum oxides.

Catalyst	A_{BET}[a] ($m^2\,g^{-1}$)	V_{tal}[b] ($mL\,g^{-1}$)	D_{avg}[c] (nm)	Density of surface hydroxyl groups ($mmol\,g^{-1}$)
HAO	119.08 ± 0.56	0.149 ± 0.003	5.00 ± 0.01	5.97
RAO	265.89 ± 1.24	0.481 ± 0.011	7.23 ± 0.004	4.55

[a] BET surface area.
[b] Total pore volume of the surface of aluminum oxides.
[c] Average diameter of pore distributed over the surface of aluminum oxides.

titration curves of HAO and RAO with different ionic strength were determined. Titration curves with different ionic strength intersected at one point, which was the pH_{pzc} of aluminum oxides [22]. In Fig. 2, it was shown clearly that pH_{pzc} were 7.26 and 8.26 for HAO and RAO, respectively. When the solution pH < pH_{pzc}, the oxide surface is electropositive. When the solution pH > pH_{pzc}, an electronegative surface is obtained [22]. The amount of adsorbed proton on the oxide surface increased with the increasing ionic strength under the same pH condition. The increasing electrolytes concentration compressed the double electric layer of solid-liquid (aluminum oxides/water). Furthermore, the reduction of electrostatic repulsion force between aluminum oxide surface and water resulted in the increase of both proton adsorption on the aluminum oxide surface and surface charge density of aluminum oxides. In aqueous solution, the surface of aluminum oxide adsorbed water molecular, leading to the surface hydroxylation. The proton-transfer reaction of surface hydroxyl group of metal oxide can be described by the acid-alkaline reaction, shown in equation (2) [22]:

$$\mathrm{MeOH_2^+} \Leftrightarrow \mathrm{MeOH} + \mathrm{H^+} \Leftrightarrow \mathrm{MeO^-} + 2\mathrm{H^+} \tag{2}$$

According to 2pK-CCM (constant capacity double-layer model) surface complexation model, the surface acid-alkaline reaction and the surface inherent acidity constants of aluminum oxides can be expressed as [22]:

$$\mathrm{AlOH_2^+} \Leftrightarrow \mathrm{AlOH} + \mathrm{H^+},$$
$$K_{a1}^s = ([\mathrm{AlOH}]^s[\mathrm{H^+}]/[\mathrm{AlOH_2^+}])\exp(-F\psi_s/RT) \tag{3}$$

$$\mathrm{AlOH} \Leftrightarrow \mathrm{AlO^-} + \mathrm{H^+}, \quad K_{a2}^s = ([\mathrm{AlO^-}]^s[\mathrm{H^+}]/[\mathrm{AlOH}])\exp(-F\psi_s/RT) \tag{4}$$

Surface inherent acidity constant (K_{a1}^s and K_{a2}^s) of aluminum oxides can be determined, and results were shown in Table 2.

3.3. *Catalyzed ozonation of MIB in water by aluminum (hydroxyl) oxides*

The removal effectiveness of catalyzed ozonation MIB in the presence of HAO or RAO was shown in Fig. 3. The removal effectiveness of MIB was only 29.1% in the sole ozonation. MIB cannot be effectively removed in short contact time (30 min) by the sole ozonation. To enhance the removal efficiency of ozonation, the catalyst (HAO or RAO) was added. However, a remarkable disparity of catalytic activity was found between HAO and RAO. HAO insignificantly enhanced the MIB removal efficiency. It only enhanced the MIB removal efficiency in the initial stages of the process (within 5 min). Nevertheless, the final removal efficiency was 27.5%, which was almost close to that of the sole ozonation. In contrast, RAO exhibited a greater catalytic activity compared with HAO. The final removal effectiveness of MIB was 98.4% within 30 min.

Table 2
pH_{pzc} and pK_{a1}^s/pK_{a2}^s of aluminum oxides.

Catalyst	pH_{pzc}	Surface inherent acidity constant, pK_{a1}^s/pK_{a2}^s
HAO	7.26	4.45/9.61
RAO	8.26	7.74/8.81

In ozonation system, the pollutants are usually decomposed by the combination of the bimolecular reactions, i.e. direct and indirect oxidation. The direct oxidation is that the pollutants directly reacted with ozone molecular. While the indirect oxidation is that the pollutants are decomposed by •OH. Catalyzed ozonation by metal oxides is regarded as an alternative method of AOPs because the enhancement of ozone decomposition by the catalyst and the generation of radical species such as •OH. The kinetics of catalyzed ozonation is assumed to be second-order or pseudo-first-order, which have been reported in several previous studies [23,24]. In this investigation, the degradation rate of MIB in both ozonation and catalyzed ozonation in the presence of HAO or RAO could be expressed as follows:

$$-\frac{d[\mathrm{MIB}]}{dt} = k_{O_3}[\mathrm{O_3}][\mathrm{MIB}] + k_{\bullet OH}[{}^\bullet\mathrm{OH}][\mathrm{MIB}] \tag{5}$$

where k_{O_3} and $k_{\bullet OH}$ were the reaction constants for ozone and •OH reacting with MIB, respectively. Equation (5) could be transformed to equation (6).

$$-\frac{d[\mathrm{MIB}]}{dt} = (k_{O_3}[\mathrm{O_3}] + k_{\bullet OH}[{}^\bullet\mathrm{OH}])[\mathrm{MIB}] \tag{6}$$

Defining $k_{app} = k_{O_3}[\mathrm{O_3}] + k_{\bullet OH}[{}^\bullet\mathrm{OH}]$, equation (6) was transformed to equation (7):

$$-\frac{d[\mathrm{MIB}]}{dt} = k_{app}[\mathrm{MIB}] \tag{7}$$

Thus, the degradation rate of MIB in both ozonation and catalyzed ozonation in the presence of HAO or RAO could be predigested as pseudo-first order. Plots of $\ln([\mathrm{MIB}]/[\mathrm{MIB}]_0)$ versus reaction time of the sole ozonation, and catalyzed ozonation by HAO or RAO were shown in Fig. 4. The fine linear fittings were observed. It was indicated that the degradation reaction of MIB in both ozonation and catalyzed ozonation followed pseudo-first order as shown in equation (7). There was a two-phase reaction in

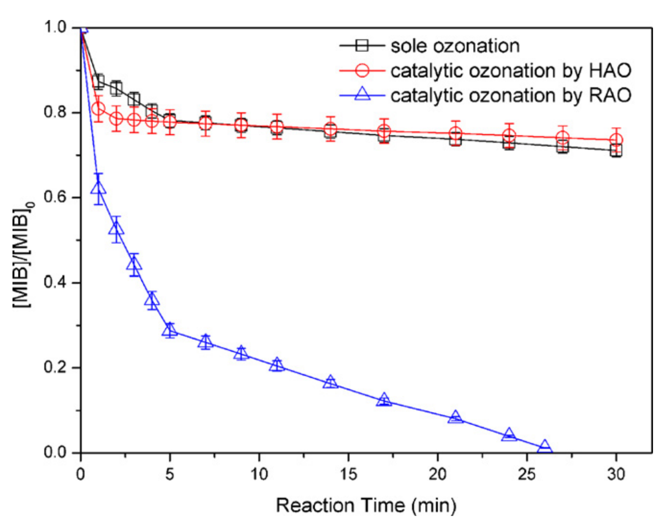

Fig. 3. Catalyzed ozonation of MIB in water by γ-AlOOH and γ-Al_2O_3. Experiment conditions: $[O_3]_0 = 0.5\,mg\,L^{-1}$, $[MIB]_0 = 23.2\,\mu g\,L^{-1}$, [catalyst] = $200\,mg\,L^{-1}$, pH 6.7 (adjusted with phosphate buffer solution ($0.1\,mmol\,L^{-1}$)).

Table 3
Pseudo-first-order rate constants of MIB degradation in the different processes.

Experiments	Kinetics constants (min^{-1})		R^2	
	The initial phase	The second phase	The initial phase	The second phase
Ozonation	0.043	3.74×10^{-3}	0.8313	0.9991
Catalytzed ozonation by HAO	0.039	2.18×10^{-3}	0.4397	0.9991
Catalytzed ozonation by RAO	0.230	79.26×10^{-3}	0.9538	0.9784

both the sole ozonation and catalyzed ozonation (Fig. 4). The initial phase, called instantaneous ozone demand (IOD), was explained by the fast consumption of ozone by organic pollutants in water or by the catalyst (HAO or RAO) [25,26]. In the IOD stage, a fast oxidation reaction between ozone and MIB took place. Ozone molecules were transformed into activated oxygen groups such as •OH that were responsible for the improvement of MIB removal effectiveness in the first phase. According to the results, the initial phase reaction (approx. 0–5 min) well fitted with pseudo-first-order kinetics. The second phase indicated a slow oxidation process. In this phase, the residual ozone molecules went on oxidizing MIB slowly. The reaction in second phase also followed pseudo-first-order kinetics. The pseudo-first-order kinetic parameters were listed in Table 3. In both two phases, RAO exhibited a better catalytic activity in catalyzed ozonation of MIB. According to the two-phase reaction theory of ozonation, some kinds of activated oxygen groups might be generated in the presence of RAO and HAO.

3.4. Inhibiting effect of tert-butyl alcohol on catalyzed ozonation

Generally, •OH was considered as the main active species in metal oxides catalyzed ozonation due to the ozone decomposition on the solid surface [12]. The generation of •OH is mainly responsible for the improvement of catalyzed ozonation. However, •OH may be not the only reason for the pollutants removal from water by catalyzed ozonation. The surface adsorption of catalysts may also play a role in pollutants removal. Ma et al. found the MnO_x/GAC catalyst could still improve the removal efficiency of nitrobenzene in the presence of radical scavengers (tert-butyl alcohol) [27]. They considered the reaction mechanism of catalyzed ozonation by MnO_x/GAC as solid surface adsorption rather than hydroxyl radical oxidation. Accordingly, radical scavenger were used to assess the possibility of •OH generation in catalyzed ozonation in the presence of HAO or RAO and to preliminarily determine the reaction mechanism in this study. It is well known that tert-butyl alcohol (TBA) is a typical •OH scavenger [28]. As seen from Fig. 5, it had remarkable inhibiting effect on the MIB removal effectiveness by RAO catalyzed ozonation. The removal efficiency of MIB sharply decreased from 98.4% to 18.0%. The result indicated •OH was the main activity species in catalyzed ozonation by RAO, and the reaction mechanism potentially followed •OH oxidation rather than solid surface adsorption. However, no significant inhibiting effect of TBA was observed in HAO catalyzed ozonation because of the less catalytic activity of HAO for MIB removal. The removal efficiency of MIB shifted from 27.5% to 25.0%. This result suggested the occurrence of the solid surface adsorption rather than the generation of •OH in the catalyzed ozonation by HAO. Therefore, the removal efficiency of MIB by HAO catalyzed ozonation was much lower. In a word, the reaction mechanism of catalyzed ozonation by HAO was dominated by solid adsorption rather than •OH oxidation. On the contrary, the catalyzed ozonation by RAO was dominated by •OH oxidation mechanism. The differences between the final removal effectiveness of MIB by different catalysts were resulted from the different reaction mechanisms.

3.5. Catalytic ozone decomposition by aluminum oxides

Generally, the inhibiting effect of tert-butyl alcohol on catalyzed ozonation was an indirect method to confirm the generation of •OH. In addition, variation of ozone decomposition rate is another indirect method to verdict whether •OH was generated in catalyzed ozonation. Variation of ozone decomposition rates in the sole ozone decomposition and catalytic ozone decomposition by aluminum oxides in the absence of MIB were shown in Fig. 6. It was observed that the ozone decomposition rates were enhanced by both HAO and RAO. This phenomenon confirmed that •OH was generated in catalytic ozone decomposition by both HAO and RAO. Especially, the improvement of ozone decomposition by HAO was

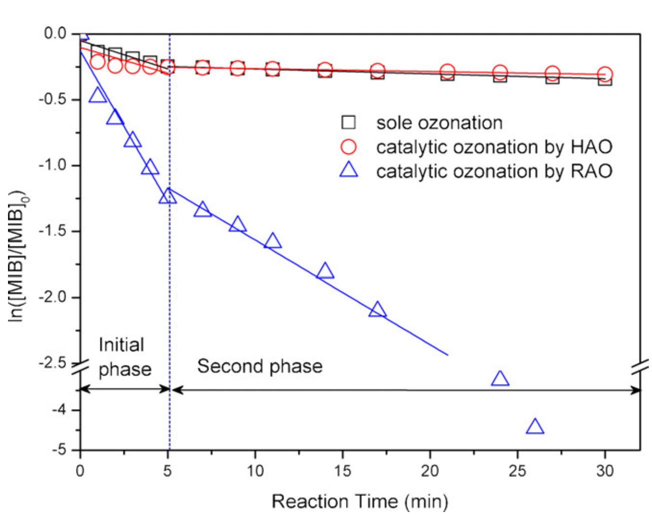

Fig. 4. Kinetics analysis of catalyzed ozonation of MIB in water. Experiment conditions: $[O_3]_0 = 0.5\ mg\ L^{-1}$, $[MIB]_0 = 23.2\ \mu g\ L^{-1}$, $[catalyst] = 200\ mg\ L^{-1}$, pH 6.7 (adjusted with phosphate buffer solution ($0.1\ mmol\ L^{-1}$)).

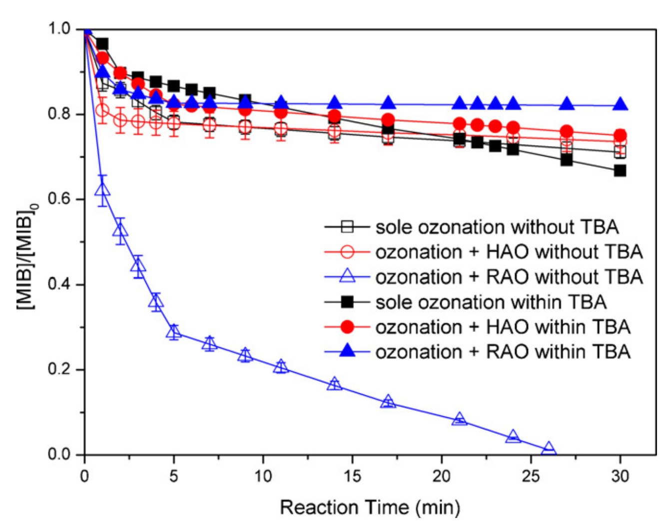

Fig. 5. Inhibiting effect of TBA on catalyzed ozonation MIB. Experiment conditions: $[O_3]_0 = 0.5\ mg\ L^{-1}$, $[MIB]_0 = 23.2\ \mu g{\cdot}L^{-1}$, $[catalyst] = 200\ mg\ L^{-1}$, $[TBA] = 1.0\ mmol\ L^{-1}$, pH = 6.7 (adjusted with phosphate buffer solution ($0.1\ mmol\ L^{-1}$)).

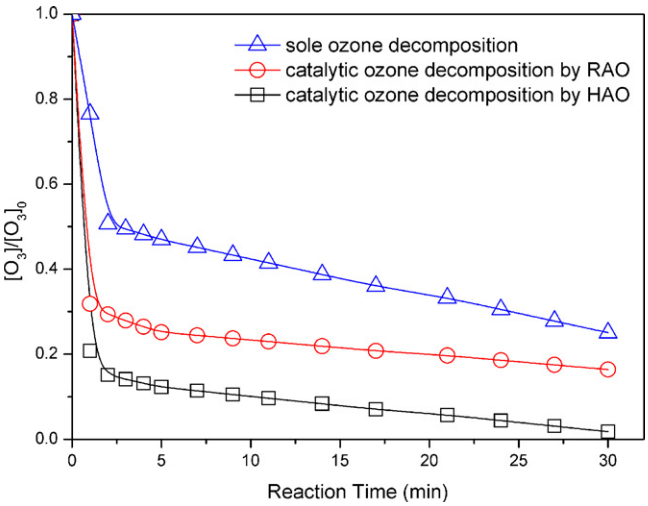

Fig. 6. Catalytic ozone decomposition by of HAO and RAO in the absence of MIB. Experiment conditions: $[O_3]_0 = 0.5\ mg\ L^{-1}$, [catalyst] = 200 mg L^{-1}, pH 6.7 (adjusted with phosphate buffer solution (0.1 mmol L^{-1})).

stronger than that of RAO. The higher ozone decomposition rate indicated more active species ($^{\bullet}$OH) generated in catalytic ozone decomposition. It was noticed that the ability of catalytic ozone decomposition by HAO was stronger than that of RAO in the absence of MIB, which made a contradiction with the results of TBA inhibiting effect. This phenomenon indicated that MIB involved in the reaction and changed the pathways of catalytic ozone decomposition by aluminum oxides, resulting in different removal efficiencies of MIB.

3.6. Role of surface hydroxyl groups on catalyzed ozonation

The surface acidity-alkalinity property determines the roles of the metal oxides in removing pollutants by adsorption [29–31], catalytic oxidation [32–34], and catalytic reduction [35]. The surface hydroxyl group is one of the most important characteristics of surface acidity-alkalinity properties. In general, the surface hydroxyl group plays an important role in adsorption [12], catalyzed ozone decomposition [36] and catalyzed ozonation [37]. According to equation (2), water pH is one of the most important factors affecting the charge status of surface hydroxyl groups of HAO and RAO. Based on surface inherent acidity constant (shown in Table 2), the species of the surface hydroxyl group under different water pH conditions can be determined (shown in Fig. 7). It is confirmed that Al-OH, Al-OH_2^+ and Al-O^- was the dominant specie of surface hydroxyl groups in the different pH ranges, respectively. The Al-OH group, of which net charge was zero, was the dominant species at water pH 7.26 for HAO, and was the dominant specie at water pH 8.26 for RAO.

Fig. 8 showed the effect of water pH on the reaction rate constants. The reaction rate constant of catalyzed ozonation by HAO or RAO was strongly pH depended. In Fig. 8, the X-axis denoted the water pH, and the Y-axis ($k_{cata} - k_{ozone}$) represented the difference between the reaction rate constant of catalyzed ozonation (k_{cata}) and that of the sole ozonation (k_{ozone}). The hydroxide ion (OH^-) is a common initiator of the chain reaction in ozone decomposition [38]. Therefore, ozone decomposition rate increases with the increasing water pH, leading to more generation of $^{\bullet}$OH. To avoid the influence of OH^- on the catalyzed ozonation, ($k_{cata} - k_{ozone}$) was used in this section. The value of ($k_{cata} - k_{ozone}$) denoted the contribution of the catalysts for MIB degradation in catalyzed ozonation under different water pH conditions.

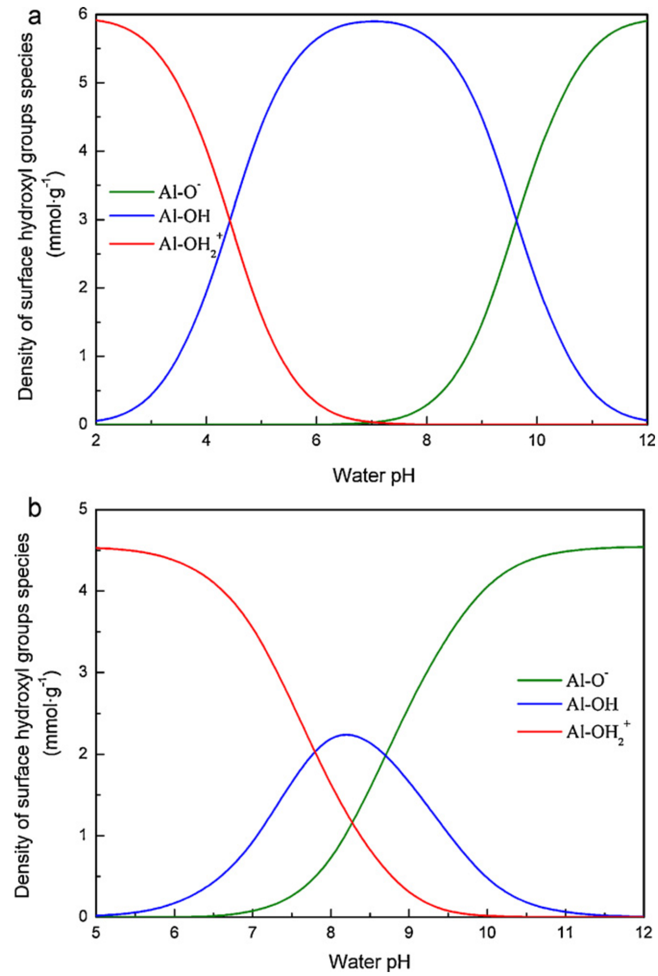

Fig. 7. Distribution of surface hydroxyl group species under different water pH conditions (a) γ-AlOOH, (b) γ-Al_2O_3.

There was an inflexion point in each curve of HAO and RAO. The inflexion point for HAO appeared around pH 7.00, while the inflexion for RAO was approximately at pH 8.20. These inflexion points showed the maximum impact of the catalyst in water pH range from 2 to 11. That was, when water pH was around 7.00

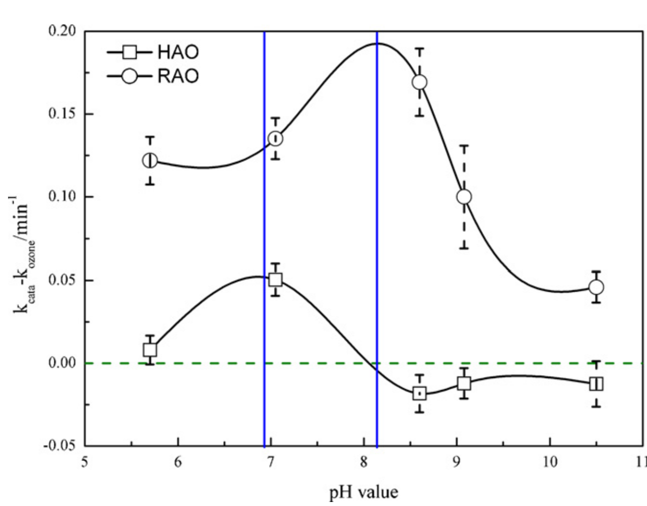

Fig. 8. Effect of water pH value on catalytic activity of aluminum oxides. Experiment conditions: $[O_3]_0 = 0.5\ mg\ L^{-1}$, $[MIB]_0 = 23.2\ \mu g\ L^{-1}$, [catalyst] = 200 mg L^{-1}, pH 6.7 (adjusted with phosphate buffer solution (0.1 mmol L^{-1})).

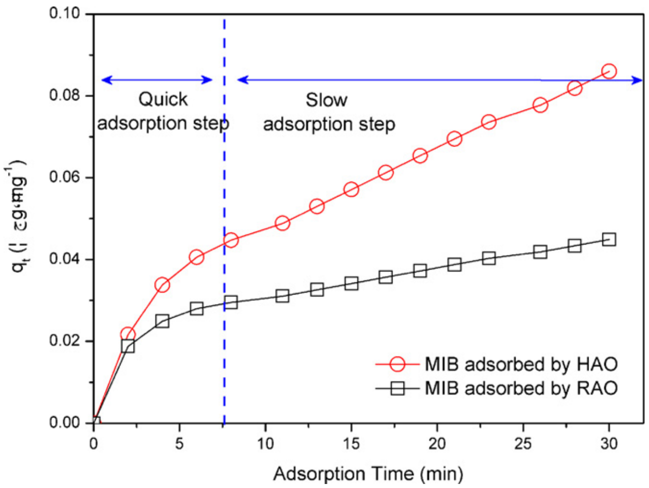

Fig. 9. Adsorption kinetics of MIB on HAO and RAO. Experiment conditions: $[MIB]_0$ = 23.2 $\mu g\,L^{-1}$, [catalyst] = 200 $mg\,L^{-1}$, pH 6.7 (adjusted with phosphate buffer solution (0.1 $mmol\,L^{-1}$)).

and 8.20, HAO and RAO had the greatest positive impact on MIB degradation, respectively. The pH_{pzc} for HAO and RAO were 7.26 and 8.26 (shown in Table 1), and they were quite close to the inflexion point in the response curve of each oxide. It was speculated that the aluminum oxides exhibited the maximum positive impact on MIB removal when water pH was closed to pH_{pzc} of itself. Because the surface charge was zero when water pH was closed to pH_{pzc} of the aluminum oxides, it was confirmed that zero charge surface of aluminum oxide was more active than electropositive and electronegative surface in catalyzed ozonation of MIB. The surface hydroxyl group was considered as the active site in catalyzed ozonation of MIB in the presence of aluminum oxides.

3.7. Adsorption mechanism of MIB on aluminum oxides

In the catalyzed ozonation, the degradation reactions are complex due to the combination of the sole ozonation, adsorption, and catalyzed ozonation [12]. Especially, it was found that the solid adsorption dominated the main reaction mechanism of catalyzed ozonation by HAO (part 3.4). Therefore, it was necessary to explain the reaction mechanism of catalyzed ozonation in presence of HAO or RAO by adsorption experiments. The investigation of MIB adsorption on the surface of aluminum oxides is helpful for further understanding the mechanism of catalyzed ozonation of MIB in the presence of aluminum oxides.

The kinetics of MIB adsorption on catalysts is illustrated in Fig. 9. The adsorption reaction could be divided into two phases, a quick adsorption step and a slow one. Quick adsorption happened in both HAO and RAO adsorption. Three adsorption kinetics models, including pseudo-second-order [39,40], Elovich equation [41] and intraparticle diffusion model [42,43] were carried out to analyze the adsorption data (results are shown in Table 4). Linear forms of these three adsorption kinetics models are presented as follows:

$$\text{Pseudo-second order equation}: \quad \frac{t}{q_t} = \frac{1}{h} + \frac{1}{q_e}t \tag{8}$$

$$h = k_2 {q_e}^2 \tag{9}$$

$$\text{Elovich model}: \quad q_t = \frac{1}{\beta}\ln(\alpha\beta) + \frac{1}{\beta}\ln(t) \tag{10}$$

$$\text{Intraparticle diffusion model}: q_t = k_p t^{1/2} + C \tag{11}$$

where q_t is the amount of MIB adsorbed on aluminum oxides per gram at any time t ($mg\,g^{-1}$); q_e is the amount of MIB adsorbed

Table 4
Kinetic parameters of MIB adsorption by HAO and RAO[a].

Catalyst	Pseudo-second order				Elovich equation			Intraparticle diffusion			
	q_e ($mg\,g^{-1}$)	k_2 ($g\,mg^{-1}\,min^{-1}$)	$h = k_2 {q_e}^2$ ($mg\,g^{-1}\,min^{-1}$)	r^2	α ($mg\,g^{-1}\,min^{-1}$)	β ($g\,mg^{-1}$)	r^2	$k_{p,1}$ ($mg\,g^{-1}\,min^{-1/2}$)	$k_{p,2}$ ($mg\,g^{-1}\,min^{-1/2}$)	${r_1}^2$	${r_2}^2$
HAO	0.11	0.802	0.00967	0.9794	0.99	43.29	0.9429	0.0164	0.0161	0.9819	0.9897
RAO	0.049	3.734	0.00929	0.9497	3.39	109.89	0.9602	0.0076	0.0060	0.9658	0.9897

Table 5
Parameters for adsorption isotherm equation of MIB adsorbed by γ-AlOOH and γ-Al_2O_3.

Isotherm model	Isotherm equation	Model constants	HAO	RAO
Langmuir	$\frac{1}{q_e}=\frac{1}{q_m K_L C_e}+\frac{1}{q_m}$	q_m (mg g^{-1})	0.9188	0.8394
		K_L (L g^{-1})	0.002823	0.00485
		r^2	0.9973	0.9898
Freundlich	$\log_{10}q_e=\frac{1}{n}\log_{10}C_e+\log_{10}K_F$	K_F [(mg g^{-1})(L mg^{-1})$^{1/n}$]	0.002574	0.005324
		n	1.0137	1.1384
		r^2	0.9923	0.9832

at equilibrium (mg g^{-1}); k_2 is the rate constant of pseudo-second order (g mg^{-1} min^{-1}); h is the initial adsorption rate of pseudo-second order (mg g^{-1} min^{-1}); α is the adsorption velocity constant for MIB (mg g^{-1} min^{-1}); β is the desorption constant (g mg^{-1}); k_p is the intraparticle diffusion constant (μg g^{-1} min$^{-1/2}$); C is the intercept of the line which is proportional to the boundary layer thickness.

The high coefficient of determination (r^2 > 0.94) confirmed that MIB adsorption on aluminum (hydroxyl) oxides was well represented by pseudo-second-order kinetics. The calculated amount of MIB adsorbed on HAO was higher than that on RAO, which indicated that MIB was more readily adsorbed by HAO. Pseudo-second-order kinetics describes the chemical adsorption on the surface of sorbent [36,37]. Elovich equation was more applicable in describing MIB adsorption on aluminum oxides with the coefficient of determination higher than 0.94. Based on results of the adsorption velocity constant (α) and desorption constant (β), it was confirmed that the adsorption velocity constants of RAO was 3.4 times higher than that of HAO, and the desorption constant of MIB on RAO was 2.53 times higher than that of MIB on HAO. This phenomenon explained the adsorption ability of HAO was higher than that of RAO. Higher adsorption and desorption constant of RAO meant that quick adsorption was observed on the surface between RAO and MIB. The adsorption equilibrium time was short, resulting in that l MIB molecule could be adsorbed or desorbed on the surface of RAO, resulting in the faint adsorption ability. This result was consistent with that of pseudo-second-order kinetics.

Due to the pore of the aluminum oxides, the intraparticle diffusion kinetic model was expected to have a role in the adsorption. Both surface adsorption and intraparticle diffusion adsorption occurred during the MIB adsorption based on the relationship between adsorption capacity and the square root of contact time [40]. Intraparticle diffusion kinetic model well described the adsorption of MIB on catalyst based on the high coefficient of determination (r^2 > 0.96). The intraparticle diffusion constant (k_p) of MIB on HAO was higher than that on RAO (Table 4), indicating the diffusion driving force of HAO was higher than that of RAO. As a result, the adsorption capacity of HAO was higher than that of RAO. The variation of adsorption capacity of aluminum oxides was contrast with the special surface area of catalyst, as well as the change of pore volume. This result confirmed that the main reason for MIB adsorption was not the intraparticle diffusion adsorption in the pores but the surface chemical adsorption on the aluminum oxides.

Langmuir [44] and Freundlich [45] adsorption isotherm equation were used to simulate adsorption isotherms of MIB adsorbed on HAO and RAO, and results were shown in Table 5. Both two adsorption isotherm equations expressed the adsorption behavior very well (r^2 > 0.98). Based on the Langmuir adsorption isotherm equation, the maximum adsorption capacity (q_m) of the adsorbents was 0.9188 μg mg^{-1} and 0.8394 μg mg^{-1} for HAO and RAO, respectively. The adsorption capacity of HAO was larger than that of RAO. However, RAO with the higher surface area did not obtain the larger adsorption capacity, which suggested the adsorption of MIB on alu-

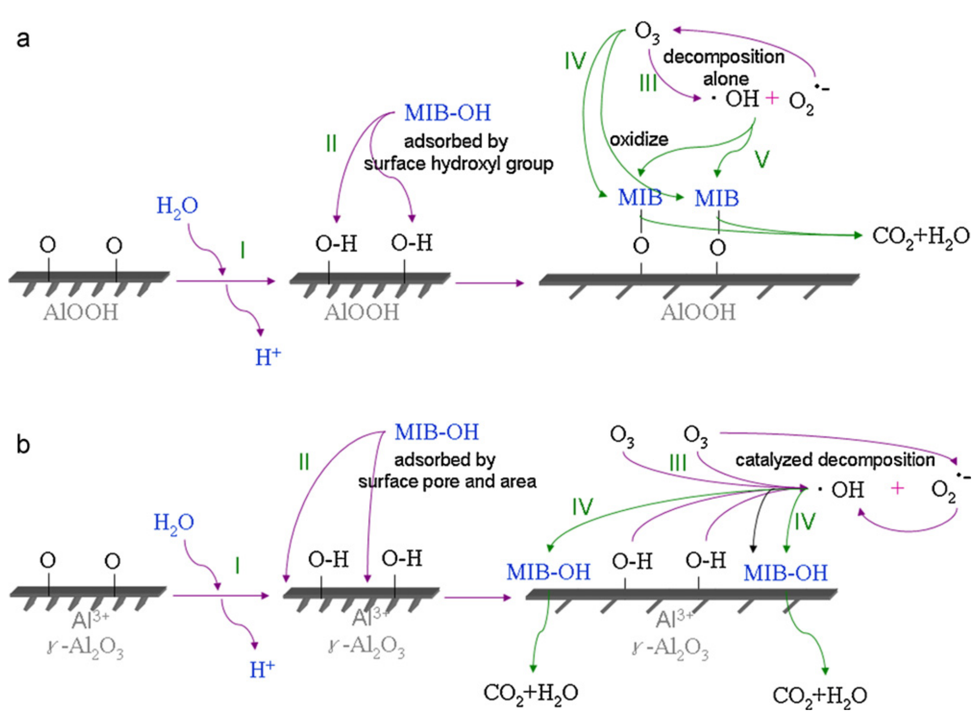

Fig. 10. Proposed catalyzed ozonation pathway in the presence of HAO or RAO. (a) HAO, (b) RAO.

minum oxides are not dominated by the surface area of aluminum oxides.

For investigation of adsorption mechanism, adsorption density (Γ_d) is defined:

$$\Gamma_d = \frac{q_m}{A} \quad (12)$$

where Γ_d is the adsorption density for MIB adsorbed on aluminum oxides ($\mu mol\, m^{-2}$); q_m is maximum adsorption capacity of adsorbent ($\mu g\, mg^{-1}$); A is BET surface area of adsorbent ($m^2\, g^{-1}$)

After calculation, Γ_d was $7.72 \times 10^{-3}\, \mu mol\, m^{-2}$ and $3.16 \times 10^{-3}\, \mu mol\, m^{-2}$ for HAO and RAO, respectively. The more density of surface hydroxyl group on HAO, the more adsorption density obtained. It was concluded that surface hydroxyl group was good for MIB adsorption. The surface hydroxyl group was the activity site of MIB adsorption on aluminum oxides.

3.8. Inhibiting effect of adsorption between surface hydroxyl group and MIB on catalyzed ozonation

Zhang et al. [37] had described the pathway of catalyzed ozonation in the presence of metal oxides by characterizing the surface property, such as pH_{pzc}, density of surface hydroxyl group, and surface Brónsted acidity. They concluded that the surface hydroxyl group played an important role in catalyzed ozonation. This result was consistent with our experimental phenomenon shown in Fig. 8. However, the lower density of surface hydroxyl groups of RAO achieved in the higher catalytic activity. Based on the analysis of part 3.6 and part 3.7, this different viewpoint can be well explained.

According to the result of part 3.6, the surface hydroxyl group was the active site for MIB ozonation catalyzed by both HAO and RAO. Moreover, the surface hydroxyl group was also the adsorption site for MIB adsorbed on aluminum oxides (as shown in part 3.7). The surface hydroxyl group was both the adsorption site and the catalytic reactive site in catalyzed ozonation. Surface hydroxyl radicals would compete to participate in catalytic ozone decomposition and MIB adsorption during MIB ozonation catalyzed by the aluminum oxides. Based on the results, MIB adsorption on HAO inhibited the generation of $^{\bullet}OH$ in catalytic ozone decomposition. This competitive reaction led to low catalytic activity of HAO in catalyzed ozonation of MIB. For RAO, though faint adsorption capacity and fast desorption rate were obtained, more $^{\bullet}OH$ were generated from the surface hydroxyl group participating in catalytic ozone decomposition, resulting in higher removal efficiency of MIB in catalyzed ozonation. Therefore, the catalytic activity of RAO was higher than HAO. The difference of catalytic activity between HAO and RAO was related to the surface hydroxyl groups and MIB adsorption on catalyst.

The possible reaction mechanism of catalyzed ozonation by aluminum oxides was proposed and illustrated in Fig. 10. When HAO and RAO were introduced into aqueous solution, water molecules were strongly adsorbed on the oxides surface, and dissociated into OH^- and H^+ to form the surface hydroxyl group (reaction I). In the catalyzed ozonation by HAO, the main reaction mechanism was solid surface domination reaction. MIB was absorbed by surface hydroxyl group on HAO (reaction II). As a result, this adsorption inhibited the generation of hydroxyl radical during the catalytic ozone decomposition caused by surface hydroxyl group on HAO. The sole ozone decomposition was account for generation of $^{\bullet}OH$ (reaction III). Both ozone (reaction IV) and few $^{\bullet}OH$ (reaction V) could oxidize MIB into CO_2 and H_2O. In the catalytic ozonation by RAO, the main reaction mechanism was hydroxyl radical reaction. MIB was absorbed by the surface and the pores of RAO (reaction II). The surface hydroxyl group on RAO initiated ozone decomposition (catalytic ozone decomposition) to generate $^{\bullet}OH$ (reaction III). Hydroxyl radicals non-selectively oxidized MIB into CO_2 and H_2O (reaction IV).

4. Conclusions

Based on above experimental results, the following conclusions can be drawn:

(1) RAO showed more significant catalytic activity than HAO in catalyzed ozonation of MIB. According to the effect of water pH on the catalytic activity, surface hydroxyl groups without surface net charge was proven as the main active reaction sites.
(2) Experiments of radical inhibition confirmed that $^{\bullet}OH$ reaction dominated the catalyzed ozonation by RAO, the catalyzed ozonation by HAO was dominated by solid surface reaction. However, both HAO and RAO can enhance ozone decomposition to generate hydroxyl radical in catalyzed ozone decomposition (without MIB). Especially, the catalytic activity of HAO was stronger than that of RAO in catalytic ozone decomposition. The inconsistent results between radical scavengers experiment and catalytic ozone decomposition were mainly because of the interaction between MIB and surface hydroxyl groups.
(3) According to the results of MIB adsorption on HAO or RAO, it was found that MIB interacted with surface hydroxyl group by chemical adsorption, and the surface hydroxyl group was the main adsorption site. HAO exhibited stronger adsorption capacity than RAO based on adsorption experiment. Quick adsorption and desorption accounted for the faint adsorption capacity of RAO.
(4) Adsorption between MIB and the surface hydroxyl group inhibited its role in catalyzed ozonation by HAO. The adsorption between MIB and the surface hydroxyl group reduced the amount of surface hydroxyl groups participating in catalytic ozone
(5) Decomposition to the generation of hydroxyl radical. This made the catalytic activity of HAO lower in the ozonation. The difference of catalytic activity between HAO and RAO was related to the surface hydroxyl groups and adsorption of MIB on catalyst.

Acknowledgements

This work was carried out with the financial support of the Fundamental Research Funds for the Central Universities (No. YX2010-25 and No. BLJC200903), and is supported by State Key Laboratory of Urban Water Resource and Environment (HIT, ES200901). China Post Doctoral Science Foundation (20100470216), Beijing Forestry University Young Scientist Fund (BLX2W8024), the National Natural Science Foundation of China (No. 40903038), and National High Technology Research and Development Program of China (No. 2008AA06Z309) also supported this research.

References

[1] K. Saito, K. Okamura, H. Kataoka, Determination of musty odorants, 2-methylisoborneol and geosmin, in environmental water by headspace solid-phase microextraction and gas chromatography-mass spectrometry, J. Chromatogr. A 1186 (2008) 434–437.
[2] K. Ozaki, A. Ohta, C. Iwata, A. Horikawa, K. Tsuji, E. Ito, Y.-K. Ikai, I. Harada, Lysis of cyanobacteria with volatile organic compounds, Chemosphere 71 (2008) 1531–1538.
[3] L. Li, N. Wan, N.Q. Gan, B.D. Xia, L.R. Song, Annual dynamics and origins of the odorous compounds in the pilot experimental area of Lake Dianchi, China, Water Sci. Technol. 55 (2007) 43–50.
[4] S. Lalezary, M. Pirbazari, M.J. McGuire, Evaluating activated carbons for removing low concentrations of taste and odour producing organics, J. Am. Water Works Assoc. 78 (1986) 62–69.
[5] J. Chesnutt, E. Thomas, M. Bach, D.W. Mazyck, Improvement of thermal reactivation of activated carbon for the removal of 2-methylisoborneol, Water Res. 41 (2007) 79–86.

[6] K. Kutschera, H. Bornick, E. Worch, Photinitiated oxidation of geosmin and 2-methylisoborneol by irradiation with 254 nm and 185 nm UV light, Water Res. 43 (2009) 2224–2232.
[7] D.W. Ferquson, M.J. McGuire, B. Koch, R.L. Wolfe, E.M. Aieta, Comparing peroxone and ozone for controlling taste and odor compounds, disinfection by-products, and microorganisms, J. Am. Water Works Assoc. 82 (1990) 181–191.
[8] E.J. Rosenfeldt, B. Melcher, K.G. Linden, UV and UV/H_2O_2 treatment of methylisoborneol (MIB) and geosmin in water, J. Water Supply Res. T. 54 (2005) 423–434.
[9] L.A. Lawton, P.K.J. Robertson, R.F. Robertson, F.G. Bruce, The destruction of 2-methylisoborneol and geosmin using titanium dioxide photocatalysis, Appl. Catal. B: Environ. 44 (2003) 9–13.
[10] W. Song, K.E. O'Shea, Ultrasonically induced degradation of 2-methylisoborneol and geosmin, Water Res. 41 (2007) 2672–2678.
[11] S. Masaki, S. Kenji, F. Hirotaka, F. Takao, S. Akiyoshi, Ozone decomposition of 2-methylisoborneol (MIB) in adsorption phase on high silica zeolites with preventing bromate formation, Water Res. 39 (2005) 2926–2934.
[12] B. Kasprzyk-Hordern, M. Ziolek, J. Nawrocki, Catalytic ozonation and methods of enhancing molecular ozone reactions in water treatment, Appl. Catal. B: Environ. 46 (2003) 639–669.
[13] F. Qi, Z.L. Chen, B.B. Xu, Z.Z. Xu, Degradation of 2-methylisoborneol in drinking water by bauxite catalyzed pzonation, J. Water Supply Res. T. 57 (2008) 427–434.
[14] F. Qi, B.B. Xu, Z.L. Chen, J. Ma, D.Z. Sun, L.Q. Zhang, F.C. Wu, Ozonation catalyzed by raw bauxite for degradation of 2, 4, 6-trichloroanisole in drinking water, J. Hazard. Mater. 168 (2009) 246–252.
[15] F. Qi, B.B. Xu, Z.L. Chen, J. Ma, D.Z. Sun, L.Q. Zhang, Influence of aluminum oxides surface properties on catalyzed ozonation of 2, 4, 6-trichloroanisole, Sep. Purif. Technol. 66 (2009) 405–410.
[16] F. Qi, B.B. Xu, Z.L. Chen, J. Ma, Catalytic ozonation for degradation of 2, 4, 6-trichloroanisole in drinking water in the presence of γ-ALOOH, Water Environ. Res. 81 (2009) 592–597.
[17] N.F. Wood, V.L. Snoevink, 2-Methylisoborneol, improved synthesis and a quantitative gas chromatographic method for trace concentrations producing odor in water, Chromatographia 132 (1977) 405–420.
[18] M Mullet, P. Fievet, A. Szymczyk, A. Foissy, J.C. Reggiani, J. Pagetti, A simple and accurate determination of the point of zero charge of ceramic membranes, Desalination 121 (1999) 41–48.
[19] H. Tamura, A. Tanaka, K.Y. Mita, R. Furrichi, Surface hydroxyl site densities on metal oxides as a measure for the ion-exchange capacity, J. Colloid Interf. Sci. 209 (1999) 225–231.
[20] H. Bader, J. Hoigné, Determination of ozone in water by the indigo method, Water Res. 15 (1981) 449–456.
[21] H.-S. Shin, H.-S. Ahn, Simple, rapid, and sensitive determination of odorous compounds in water by GC–MS, Chromatographia 59 (2004) 107–113.
[22] W Stumm, Chemistry of the Solid–Water Interface, Wiley & Sons Inc., New York, 1992.
[23] L. Zhao, J. Ma, Z. Sun, X. Zhai, Preliminary kinetic study on the degradation of nitrobenzene bymodified ceramic honeycomb-catalytic ozonation in aqueous solution, J. Hazard. Mater. 161 (2009) 988–994.
[24] Y. Yang, J. Ma, Q. Qin, X. Zhai, Degradation of nitrobenzene by nano-TiO_2 catalyzed ozonation, J. Mol. Catal. A: Chem. 267 (2007) 41–48.
[25] C.L. Bianchi, C. Pirola, V. Ragaini, E. Selli, Mechanism and efficiency of atrazine degradation under combined oxidation processe, Appl. Catal. B: Environ. 64 (2006) 131–138.
[26] H.N. Lim, H. Choi, T.W. Hwang, J.W. Kang, Characterization of ozone decomposition in a soil slurry: kinetics and mechanism, Water Res. 36 (2002) 219–229.
[27] J. Ma, M.H. Sui, T. Zhang, C.Y. Guan, Effect of pH on MnOx/GAC catalyzed ozonation for degradation of nitrobenzene, Water Res. 39 (2005) 779–786.
[28] J. Staehelin, J. Hoigné, Decomposition of ozone in water in the presence of organic solutes acting as promoters and inhibitors of radical chain reactions, Environ. Sci. Technol. 19 (1985) 1206–1213.
[29] H. Zeng, M. Arashiro, D.E. Giammar, Effects of water chemistry and flow rate on arsenate removal by adsorption to an iron oxide-based sorbent, Water Res. 42 (2008) 4629–4636.
[30] K. Biswas, K. Gupta, U.C. Ghosh, Adsorption of fluoride by hydrous iron(III)-tin(IV) bimetal mixed oxide from the aqueous solutions, Chem. Eng. J. 149 (2009) 196–206.
[31] K. Ada, A. Ergene, S. Tan, E. Yalçın, Adsorption of remazol brilliant blue r using zno fine powder: equilibrium, kinetic and thermodynamic modeling studies, J. Hazard. Mater. 165 (2009) 637–644.
[32] R. Gonzalez-Olmos, U. Roland, H. Toufar, F.-D. Kopinke, A. Georgi, Fe-zeolites as catalysts for chemical oxidation of MTBE in water with H_2O_2, Appl. Catal. B: Environ. 89 (2009) 356–364.
[33] L. Zhao, J. Ma, Z. Sun, H. Liu, Mechanism of heterogeneous catalytic ozonation of nitrobenzene in aqueous solution with modified ceramic honeycomb, Appl. Catal. B: Environ. 89 (2009) 326–334.
[34] W. Li, S. Zhao, B. Qi, Y. Du, X. Wang, M. Huo, Electrocatalytic reduction of chromium by poly(aniline-co-o-aminophenol): an efficient and recyclable way to remove Cr(VI) in wastewater, Appl. Catal. B: Environ. 92 (2009) 333–340.
[35] A.J. Frierdich, C.E. Joseph, T.J. Strathmann, Catalytic reduction of n-nitrosodimethylamine with nanophase nickel-boron, Appl. Catal. B: Environ. 90 (2009) 175–183.
[36] F. Qi, Z.L. Chen, B.B. Xu, J.M. Shen, J. Ma, C. Joll, A. Heitz, Influence of surface texture and acid-base properties on ozone decomposition catalyzed by aluminum(hydroxyl) oxides, Appl. Catal. B: Environ. 84 (2008) 684–690.
[37] T. Zhang, C. Li, J. Ma, H. Tian, Z. Qiang, Surface hydroxyl groups of synthetic α-FeOOH in promoting ·OH generation from aqueous ozone: Property and activity relationship, Appl. Catal. B: Environ. 82 (2008) 131–137.
[38] U. Von Gunten, Ozonation of drinking water: Part I. Oxidation kinetics and product formation, Water Res. 37 (2003) 1443–1463.
[39] Y.S. Ho, G. McKay, Kinetic models for the sorption of dye from aqueous solution by wood, Process Safety Environ. Protect. 76 (1998) 183–191.
[40] Y.S. Ho, G. McKay, The kinetics of sorption of divalent metal ions onto sphagnum moss peat, Water Res. 34 (2000) 735–742.
[41] S.H. Chien, W.R. Clayton, Soil Sci. Soc. Am. J. 44 (1980) 265–268.
[42] W.J. Weber Jr., J.C. Morriss, Kinetics of adsorption on carbon from solution, J. Sanit. Eng. Div. Am. Soc. Civil Eng. 89 (1963) 31–60.
[43] M.A. Al-Ghouti, M.A.M. Khraisheh, M.N.M. Ahmad, S. Allen, Adsorption behaviour of methylene blue onto Jordanian diatomite: a kinetic study, J. Hazard. Mater. 165 (2009) 589–598.
[44] I. Langmuri, The adsorption of gases on plane surfaces of glass, mica and platinum, J. Am. Chem. Soc. 40 (1918) 1361–1368.
[45] H.M.F. Freundlich, Uber die adsorption in lusungen, J. Phys. Chem. 57 (1906) 385–470.